Forschungszentrum Karlsruhe
in der Helmholtz-Gemeinschaft

STRATOSPHERIC AEROSOL OPTICAL DEPTH, MASS, AND SURFACE AREA: LIDAR OBSERVATIONS AT GARMISCH-PARTENKIRCHEN SINCE 1976

H. Jäger, F. Homburg, H. Giehl, and T. Deshler*

Institut für Meteorologie und Klimaforschung, Bereich Atmosphärische Umweltforschung (IMK-IFU), Forschungszentrum Karlsruhe, D-82467 Garmisch-Partenkirchen, Germany

*Department of Atmospheric Science, University of Wyoming, Laramie, WY 82071, USA

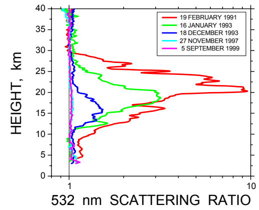

Figure 1. Lidar profiles (scattering ratio = ratio of observed total to calculated molecular backscatter).

INTRODUCTION Lidar remote sensing has proven to be invaluable in detecting and monitoring the occurrence, magnitude, spread, and decay of volcanic eruption clouds perturbing the stratospheric sulfate aerosol layer. Observations at the northern midlatitude NDSC (Network for the Detection of Stratospheric Change) station Garmisch (47.5°N, 11.1°E) have contributed to the understanding of the stratosphere since 1976. Major global perturbations observed were caused by the equatorial eruptions of El Chichon (Mexico) in 1982 and Pinatubo (Philippines) in 1991. Besides these events additional eleven eruption clouds could be detected since 1979, their atmospheric effects ranging from global to hemispheric and regional. The lidar profiles of Figure 1 present the range of high volcanic to background condition after the Pinatubo eruption. The time series of integrated backscatter measured by lidar since 1976 (Figure 2) also includes observations during three stratospheric background periods, 1976/79, 1988/90, and the present.

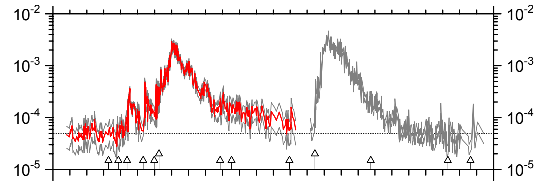

Figure 2. Stratospheric column particle backscatter at 694.3 nm with uncertainty range measured by lidar at Garmisch-Partenkirchen (tropopause + 1 km to layer top).

LIDAR CONVERSIONS Lidar backscatter profiles are converted to parameters important in understanding the impact of stratospheric aerosols on the atmospheric radiation budget and heterogeneous chemical processes: particle optical depth, mass, and surface area concentration. The method utilizes particle size distributions derived from monthly measurements with balloonborne optical particle counters at Laramie, Wyoming, 41°N [Deshler et al., 1993; Deshler and Oltmans, 1998].

Stratospheric background aerosols are characterized by lognormal size distributions peaking at radii <0.1 µm, which can be regarded monomodal. In the case of high volcanic load the distribution is moved to towards greater radii and can better be described by a bimodal lognormal distribution (Figure 3).

0.01

Figure 3. Aerosol size distributions derived from balloonborne measurements above Laramie at an altitude of 20 km.

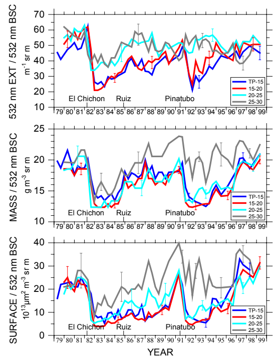

Figure 4. Particle extinction, mass, and surface area to backscatter conversion factors at 532 nm in four height ranges.

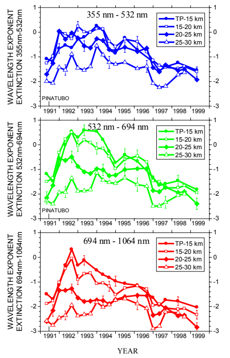

Figure 5. Wavelength exponents for particle extinction between 355 and 1064 nm in four height ranges.

RESULTS Ratios of particle extinction, mass, and surface area to particle backscatter (Figure 4), and wavelength dependences of particle backscatter and extinction (Figure 5) are calculated in four height ranges applying Mie calculations of light scattering and extinction [Jäger and Hofmann, 1991; Jäger et al., 1995; Jäger and Deshler, 2002]. These calculations can be exercised for spherical particles with known refractice index (1.44 to 1.45), specific gravity (1.65 to 1.80 g cm^{-3}), and size distribution. These parameters exclude temperatures below -70°C, and regions with elevated water vapor pressure close to the tropopause.

The conversions decrease after El Chichon and Pinatubo, reaching a minimum in the year following each eruption (Figure 4). Extended background periods can be noticed prior to El Chichon and since about 1997. The recovery after El Chichon is slowed compared to after Pinatubo, probably due to the perturbations of Ruiz (1985) and/or Nyamuragira (1986), so that background conditions were not reached until just before the Pinatubo event. The wavelength exponents were calculated for three wavelenth intervals 355-532 nm, 532-694 nm and 694-1064 nm. They increase after Pinatubo and return to background conditions beginning in 1997 (Figure 5).

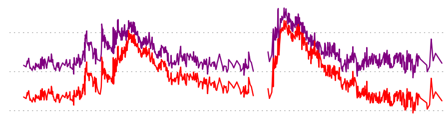

Figure 6. Column surface, 694 nm optical depth, and column mass of the stratospheric aerosol derived from lidar backscatter measurements at Garmisch-Partenkirchen.

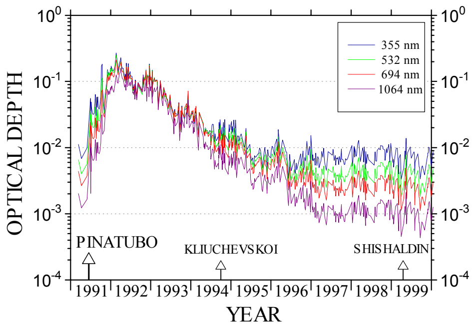

Figure 7. Optical depth of the stratospheric aerosol layer at four wavelengths derived from lidar backscatter measurements at 532 nm (tropopause to layer top).

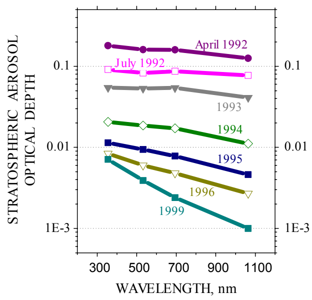

Figure 8. Mean aerosol optical depth at high, medium and low stratospheric load derived from lidar backscatter measurements at 532 nm.

APPLICATIONS The above conversions were applied to lidar backscatter measurements at Garmisch-Partenkirchen. Figure 6 shows time series beginning in 1976 of aerosol optical depth (694 nm), column surface, and column mass. The variation of the optical depth at four wavelenghts (355, 532, 694, and 1064 nm) is presented in Figure 7 for the period 1991 to 1999. Figure 8 shows the wavelength dependence of the aerosol optical depth after the Pinatubo event. There is only minimal wavelength dependence at the maximum Pinatubo perturbation in 1992, indicating that large particles cause an almost zero dependence over the visible spectral range. Thereafter, as large particles diminish in the stratosphere, the wavelength dependence increased to an almost quadratic characteristic for the 1999 average background aerosol.

CONCLUSIONS The results show that the interpretation of lidar backscatter from the stratosphere with respect to aerosol parameters might not be trivial after major volcanic eruptions and may be strongly influenced by low concentrations of large particles. Two factors play a role: the mass of volcanic sulfate aerosol forming in the stratosphere after an eruption, and the closeness of the eruption to the equator. Equatorial eruptions result in a longlasting perturbation usually of both hemispheres. The slow transport towards the polar sink of stratospheric air provides time for the formation of a significant fraction of large particles leading to effects observed over many years.

REFERENCES

Deshler, T., B.J. Johnson, and W.R. Rozier, Balloonborne measurements of Pinatubo aerosol during 1991 and 1992 at 41°N: vertical profiles, size distribution, and volatility, Geophys. Res. Lett., 20, 1435-1438, 1993.

Deshler, T., and S.J. Oltmans, Vertical profiles of volcanic aerosol and polar stratospheric clouds above Kiruna, Sweden: Winters 1993 and 1995, J. Atmos. Chem., 30, 11-23. 1998.

Jäger, H., and D. Hofmann, Midlatitude lidar backscatter to mass, area, and extinction conversion model based on in situ aerosol measurements from 1980 to 1987, Appl. Opt.30, 127-138, 1991.

Jäger, H., T. Deshler, and D.J. Hofmann, Midlatitude lidar backscatter conversions based on balloonborne aerosol measurements, Geophys. Res. Lett. 22, 1729-1732, 1995.

Jäger, H., and T. Deshler, Lidar backscatter to extinction mass and area conversions for stratospheric aerosols based on midlatitude balloonborne size distribution measurements, accepted by Geophys.Res. Lett., July 2002.

ACKNOWLEDGMENTS. The research at IFU has been supported by the German Bundes-ministerium für Bildung, Wissenschaft, Forschung und Technologie (AFS Lidar Network) and by the Commission of the European Union (EARLINET). The research at Laramie has been supported by the National Science Foundation.

E mail: horst.jaeger@imk.fzk.de deshler@uwyo.edu